

Article

Trimethoxy Silyl End-Capped Hyperbranched Polyglycidol/Polycaprolactone Particle Gels for Cell Delivery and Tissue Repair: Mechanical Properties, Biocompatibility, and Biodegradability Studies

Clara González-Chomón ¹, Vasil M. Garamus ² , Judith Hoyland ³ and Silvia S. Halacheva ^{4,*} 

¹ Institute for Materials Research and Innovation, University of Bolton, Deane Road, Bolton BL3 5AB, UK; claragchomon@hotmail.com

² Helmholtz-Zentrum Hereon, Max-Planck-Str., 21502 Geesthacht, Germany; vasy1.haramus@hereon.de

³ School of Biological Sciences, The University of Manchester, Oxford Rd, Manchester M13 9PL, UK; judith.a.hoyland@manchester.ac.uk

⁴ Faculty of Medicine and Health Sciences, The University of Buckingham, Crewe Campus, Crewe Green Road, Crewe, Cheshire CW1 5DU, UK

* Correspondence: silviya.halacheva@buckingham.ac.uk; Tel.: +44-(0)1280-827603

Abstract: This study focuses on the development of new biocompatible and biodegradable particle gel scaffolds based on PCL-HBPG/1SiHBPG triblock copolymers composed of a polycaprolactone (PCL) core and two outer blocks of trimethoxysilyl end-capped hyperbranched polyglycidol (HBPG/1SiHBPG) that have the potential to be used in soft tissue regeneration. The relationship between the gel's composition, structure, mechanical properties, and performance has been investigated for the first time and the copolymer design parameters have been optimized. The particle gel scaffolds were formed from the concentrated dispersions of the most hydrophobic PCL-45HBPG/1SiHBPG at low temperatures, and were the result of the numerous hydrogen bonds formed from the HBPG/1SiHBPG moieties as well as the formation of siloxane crosslinks (i.e., Si–O–Si bonds). These gels were formed in the physiological temperature range. Gels with a mechanical strength that gradually increases were formed from the physically crosslinked PCL-45HBPG/1SiHBPG particles effectively and safely, in the absence of UV radiation. They feature high elasticity and undergo enzyme-triggered disassembly. The gels are biocompatible and have the potential to invoke cell attachment and differentiation in the absence of exogenous biological stimuli. A successful outcome of this study will be the prospect of a new approach for tissue regeneration that is currently not available.

Keywords: copolymers; siloxane crosslinks; biocompatibility; biodegradability; gel scaffolds; soft tissue regeneration; physical crosslinking; SAXS; rheology



Citation: González-Chomón, C.; Garamus, V.M.; Hoyland, J.; Halacheva, S.S. Trimethoxy Silyl End-Capped Hyperbranched Polyglycidol/Polycaprolactone Particle Gels for Cell Delivery and Tissue Repair: Mechanical Properties, Biocompatibility, and Biodegradability Studies. *J. Compos. Sci.* **2023**, *7*, 451. <https://doi.org/10.3390/jcs7110451>

Academic Editor: Francesco Tornabene

Received: 18 September 2023

Revised: 15 October 2023

Accepted: 24 October 2023

Published: 31 October 2023



Copyright: © 2023 by the authors. Licensee MDPI, Basel, Switzerland. This article is an open access article distributed under the terms and conditions of the Creative Commons Attribution (CC BY) license (<https://creativecommons.org/licenses/by/4.0/>).

1. Introduction

Hydrogels are hydrophilic polymer networks which can retain a significant amount of water or biological fluid in their three-dimensional structure but that do not dissolve. Their use in various biomedical applications has been researched extensively due to their biocompatibility, polyfunctionality, stimuli responsiveness, and physical properties which resemble those of the native extracellular matrix (ECM) [1]. A significant number of studies have addressed the use of polymer-based smart hydrogels as a biomimetic scaffold that provides a similar microenvironment to the ECM while featuring adjustable mechanical and chemical properties [2,3]. The polymer scaffolds can be designed to be biodegradable or bioresorbable for complete elimination from the body without the need for secondary intervention [4]. Synthetic polymers such as Pluronic[®], poly(ethylene glycol)-polycaprolactone—poly(ethylene glycol), and poly(l-glutamic acid), have been successfully

utilized for the development of these scaffolds [5–8]. Hydrogels can either be prepared via chemical or physical crosslinking. Physical hydrogels are spontaneously formed by relatively weak interactions such as hydrophobic interactions or hydrogen bonding, whereas chemical hydrogels are most often formed by much stronger covalent crosslinks. The development of physically self-crosslinked polymer scaffolds, which do not require the use of a crosslinker or catalyst, has been the subject of a great number of studies [9].

Recently, polymer scaffolds based on hydrophilic hyperbranched polyglycidol (HBPG) have attracted significant attention in tissue engineering because of their high functionality, desirable mechanical properties, solubility in aqueous media, and biocompatibility [10]. The multiple pendant hydroxyl groups of HBPG provide opportunities for attachment to targeted biological cells and tissues and enhance the ability of the material to support cell adhesion and differentiation [11–13]. Wu et al. [14] utilized horseradish peroxidase for the oxidative crosslinking of a hyperbranched polyglycerol functionalized with phenol groups. The obtained materials were biocompatible and showed good potential for the encapsulation of living cells for regenerative therapy. Haryanto et al. [15] developed a microporous hydrogel scaffold from hyperbranched polyglycidol and poly(ethylene oxide) using electron-beam-induced crosslinking for tissue engineering applications. The scaffold showed good potential for use as a matrix for cellular attachment and proliferation. Li et al. [12] developed a supramolecular hydrogel (AD-g-HPG/CD-g-Dex) based on dextran and hyperbranched polyglycerol using the interaction between adamantane and β -cyclodextran. The hydrogels showed controlled encapsulate-and-release behavior and were cytocompatible. De Queiros et al. [13] fabricated a novel bone scaffolding material by electrospinning hydroxyapatite nanoparticles containing solutions of hyperbranched polyglycerol. The scaffolds were found to promote cell adhesion and proliferation.

Polymer scaffolds based on trimethoxysilyl-containing polymers such as 3-(trimethoxy silyl) propyl methacrylate have also been developed and studied for tissue engineering applications [16]. Trimethoxysilyl-containing polymers and their composites have a long-established role in the production of functional nanoscale coatings [17,18], solid polymer electrolytes [19], controlled drug release, and non-destructive cell harvesting [20–23]. Our previous research focused on the synthesis and characterization of novel triblock copolymers, which were composed of a central block of hydrophobic PCL flanked by two blocks of hydrophilic HBPG and trimethoxysilyl HBPG (SiHBPG) copolymers [24].

The copolymers' compositions are described in their names: the numbers preceding HBPG and SiHBPG refer to the average number of moles of glycidol and 3-(trimethoxysilyl) glycidol monomers, respectively, present relative to the moles of caprolactone monomers in each polymer. The number preceding PCL has been omitted for clarity and conciseness and is the remainder in each case. For example, PCL-90HBPG/1SiHBPG contains 90 mol% glycidol, 1 mol% 3-(trimethoxysilyl)glycidol, and 9 mol% caprolactone units. These proportions have been determined by ^1H NMR and elemental analyses [24].

The mean DP of the HBPG blocks in HBPG/1SiHBPG, PCL-45HBPG/1SiHBPG, PCL-56HBPG/1SiHBPG, PCL-73HBPG/1SiHBPG, and PCL-90HBPG/1SiHBPG are 54, 22, 34, 73, and 242, respectively. Each of these properties was determined by ^1H NMR in $\text{DMSO-}d_6$. Elemental analyses confirmed the expected weight percentages of silicon [24].

At higher concentrations than their corresponding critical aggregation concentration, in aqueous solution, the PCL-HBPG/1SiHBPG copolymers spontaneously self-assemble into big multicore structures comprised of PCL domains with HBPG/1SiHBPG corona. The particles were stabilized by hydrogen bonding between the HBPG moieties as well as via formation of siloxane crosslinks. The particles which formed from the most hydrophilic copolymers were only slightly affected by an increase in temperature, whereas at elevated temperatures the particles formed from the more hydrophobic copolymers became tighter and more compact.

Herein, we investigate the potential of the novel PCL-HBPG/1SiHBPG copolymers to form gel scaffolds which can be covalently crosslinked via the gradual hydrolysis of trimethoxysilyl groups to form silanol moieties that subsequently condense intermolecu-

larly via siloxane bond (Si–O–Si) formation, crosslinking the material [25]. Hydrolysable alkoxy silanes are frequently used as coupling agents due to their favorable rates of hydrolysis and subsequent formation of siloxane-based crosslinks [26]. Understanding the relationship between the chemical structure of the copolymers, their aqueous solution behavior, and their macroscopic properties is crucial for developing gel scaffolds with a targeted range of properties for any specific application.

The mechanical properties of the PCL-HBPG/1SiHBPG gels were explored over time and compared in terms of the particle structure and composition. The biocompatibility and the enzyme-triggered disassembly of the scaffolds were studied as a function of the scaffold's composition and structure. A range of complementary characterization methods have been utilized, including dynamic rheology, small-angle X-ray scattering (SAXS), and optical microscopy.

2. Results

2.1. Mechanical Properties of Gels

2.1.1. Frequency-Sweep Data

Dynamic rheology measurements were carried out using 1 mg/mL of the PCL-HBPG/1SiHBPG particle dispersions at temperatures between 20 and 70 °C. The frequency-sweep studies were carried out at 0.1–100 Hz and at a constant strain of 0.1%. The variations in G' and G'' with the oscillatory frequencies for PCL-45HBPG/1SiHBPG, PCL-90HBPG/1SiHBPG, PCL-56HBPG/1SiHBPG, PCL-73HBPG/1SiHBPG at 20 °C are shown in Figure 1. For all systems except that of PCL-45HBPG/1SiHBPG very low moduli values were observed. The solutions of PCL-90HBPG/1SiHBPG, PCL-56HBPG/1SiHBPG, and PCL-73HBPG/1SiHBPG behaved as fluids, with a loss modulus, G'' , larger than the storage modulus, G' . Compared to the rest of the copolymers, where a flow zone was observed over the whole frequency range tested, the solution of PCL-45HBPG/1SiHBPG showed gel-like behavior, with a storage modulus greater than the loss modulus (Figure 1). Furthermore, for the PCL-45HBPG/1SiHBPG solution, the magnitudes of the moduli were found to be considerably greater than the moduli of the solutions of the rest of the copolymers.

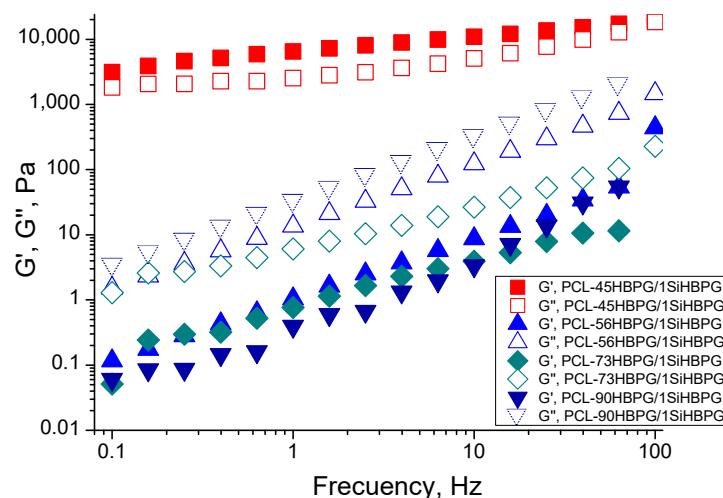


Figure 1. Variations in G' and G'' with frequency for all polymers; studied at 20 °C.

2.1.2. Strain-Sweep Data

Strain-sweep dynamic rheology experiments were carried out with the PCL-HBPG/1SiHBPG solutions at two temperatures and at a constant frequency of 1 Hz. The strain-sweep data for PCL-45HBPG/1SiHBPG at 20 °C and 37 °C are shown in Figure 2. For the remaining PCL-HBPG/1SiHBPG solutions, the data at 20 °C are presented in Figure 3. At low strain (γ), i.e., less than 10%, and at low temperature, the dispersion of PCL-45HBPG/1SiHBPG showed an elastic response, with $G' > G''$, whereas at higher deformations the response was clearly not elastic. For the PCL-45HBPG/1SiHBPG solution,

the increase in temperature resulted in decreases in both G' and G'' . Throughout the strain range studied the concentrated dispersions of the remaining polymers showed fluid-like behavior, with $G'' > G'$; see Figure 3.

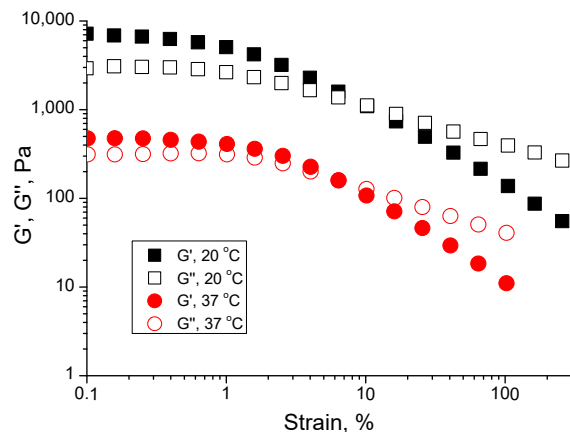


Figure 2. Variations in G' and G'' with the strain % for PCL-45HBPG/1SiHBPG at 20 °C and 37 °C.

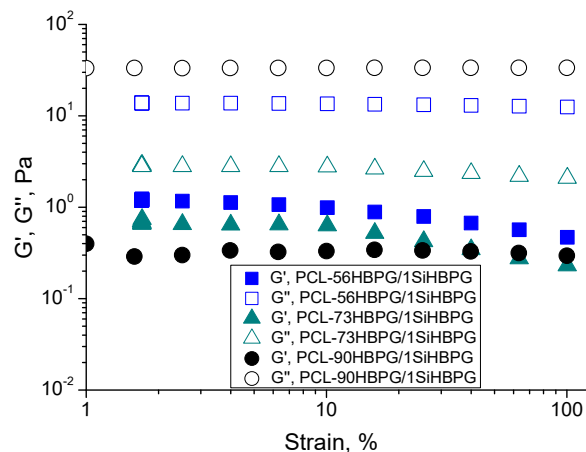


Figure 3. Variations in G' and G'' with the strain % for PCL-56HBPG/1SiHBPG, PCL-73HBPG/1SiHBPG, and PCL-90HBPG/1SiHBPG at 20 °C.

2.1.3. Temperature-Sweep Data

The rheological properties of the copolymer' aqueous solutions were investigated as a function of temperature. A frequency of 0.1 Hz and a rate of heating of 1 °C/min were the conditions used for the viscoelastic measurements. The variations in the storage and loss moduli with temperature for all copolymers studied are shown in Figure 4. The patterns of the curves resemble those which were previously observed for other amphiphilic block copolymer systems [27]. For the PCL-45HBPG/1SiHBPG solution, the fully developed evolution of the moduli displays three distinct regions (Figure 4a): (i) a low-temperature region in which the moduli do not change significantly; (ii) a narrow interval with a sharp decrease; and (iii) a high-temperature region where the moduli values reach a plateau. At temperatures below 30 °C the solution shows elastic behavior, with $G' > G''$. As the temperature increases, the moduli values sharply decrease, and at temperatures of approximately 38 °C a crossover is observed, at which $G'' > G'$. As the temperature increases further the liquid-like behavior becomes predominant.

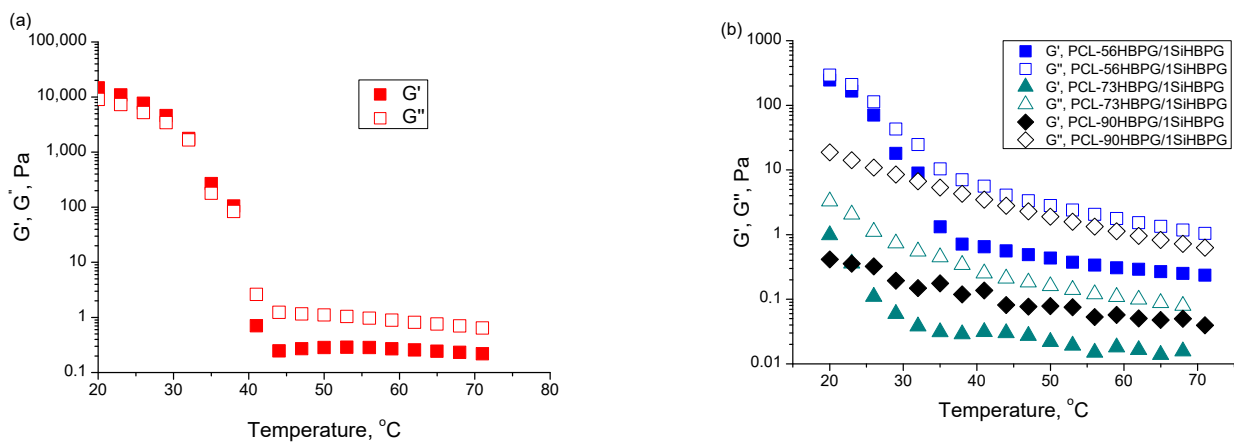


Figure 4. Variations in G' and G'' with temperature for (a) PCL-45HBPG/1SiHBPG and (b) PCL-56HBPG/1SiHBPG, PCL-73HBPG/1SiHBPG, and PCL-90HBPG/1SiHBPG.

In contrast to the PCL-45HBPG/1SiHBPG solution, the more hydrophilic PCL-56HBPG/1SiHBPG, PCL-73HBPG/1SiHBPG and PCL-90HBPG/1SiHBPG solutions behave as fluids over the entire temperature range tested, with $G'' > G'$ (Figure 4b). For these systems, there is a sharp initial decrease in the moduli values at lower temperatures and the occurrence of plateau regions at higher temperatures.

2.2. Covalent Crosslinking of the PCL-HBPG/1SiHBPG Particle Dispersions

The crosslinking of polymers is an important process for improving the stability, toughness, and mechanical elasticity of polymeric gels [4].

Alkoxysilanes have been previously used extensively in sol-gel preparation methods [28,29]. The alkoxy groups of trimethoxysilane hydrolyze in aqueous solutions to form silanol-containing species ($-SiOH$), which are highly reactive and responsible for the formation of the $Si-O-Si$ bond via a subsequent condensation reaction. The silanol-containing moieties are unstable and readily condense with themselves or with alkoxysilanes to form siloxanes. During our studies, the hydrolysis of trimethoxysilyl groups is expected to commence immediately upon the polymer's contact with water, with the inevitable condensation reactions, to form inter- and inraparticle siloxane linkages, occurring at a progressively faster rate as the concentration of silanol moieties increases [25,30].

For the concentrated dispersion of PCL-HBPG/1SiHBPG, inter- and intra-shell crosslinking of the copolymer particles could result from the gradual hydrolysis of the trimethoxysilyl groups, which generate silanol moieties that readily condense to form strong $Si-O-Si$ bonds, thereby crosslinking the particles (Figure 5).

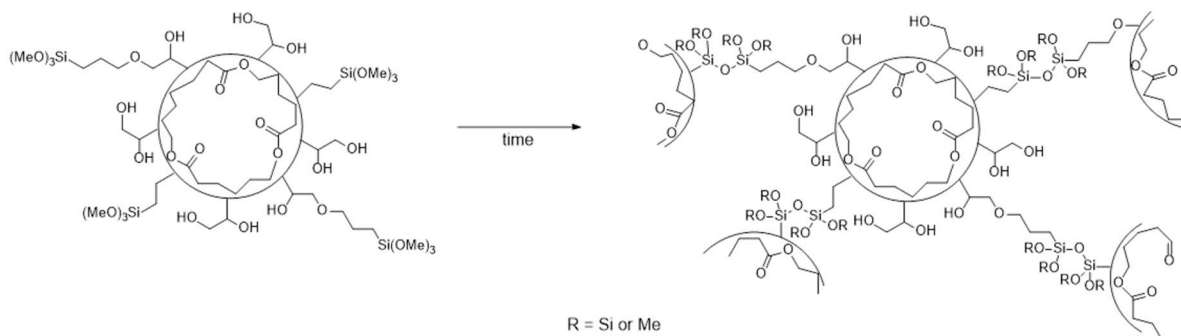


Figure 5. PCL-HBPG/1SiHBPG hydrogel formation.

Time-Sweep Rheological Data

The potential of the PCL-HBPG/1SiHBPG to form particle gel scaffolds because of the gradual hydrolysis of the trimethoxysilyl groups and Si–O–Si bond formation was tested using dynamic rheology over time at a constant strain. The time-sweep rheology can be an effective tool to monitor the gelation with time and the possible phase transitions, such as a sol-to-gel transition [31]. The measurements were performed with all copolymer dispersions at a concentration of 1 mg/mL, a constant frequency of 1 Hz, and strain of 0.1%, 24 h after the polymers were mixed with water. The extent of crosslinking was calculated assuming that every single trimethoxysilyl end group of the SiHBPG will hydrolyze in water and form at least one Si–O–Si bond with another trimethoxysilyl end group. Therefore, the minimum concentration of the crosslinks will be half of the concentration of the trimethoxysilyl groups, as previously reported [24]. Accordingly, the HBPG/1SiHBPG, PCL-45HBPG/1SiHBPG, PCL-56HBPG/1SiHBPG, PCL-73HBPG/1SiHBPG, and PCL-90HBPG/1SiHBPG contain crosslinks at levels of 0.4, 0.5, 0.5, 0.7, and 0.3 mol%, respectively.

For the PCL-45HBPG/1SiHBPG, the storage and elastic moduli were measured as a function of time at temperatures of 20, 37, and 60 °C, as shown in Figure 6. At 20 and 37 °C, the mechanical response of PCL-45HBPG/1SiHBPG was elastic, with $G' > G''$, and showed a plateau at the beginning of the experiment. A steady increase in the gel's elasticity was seen with time and could be attributed to the gradual crosslinking of the trimethoxysilyl groups. As the crosslinking became more extensive, the molecular weight of the polymers increased, which in turn increased both the relative contribution of the elastic modulus G' and the viscosity. Increasing the temperature from 20 to 60 °C resulted in a decrease in the magnitudes of the moduli. The most pronounced was the decrease in the G'' and G' values at 60 °C, where an occurrence of the flow zone with a loss modulus, G'' , larger than the storage modulus, G' , was also observed. This finding is consistent with the increase in the solubility of the HBPG moieties as the temperature increases [24]. The extent of the crosslinking is clearly not enough to overcome the HBPG dissolution in the particles' shells as the temperature increases.

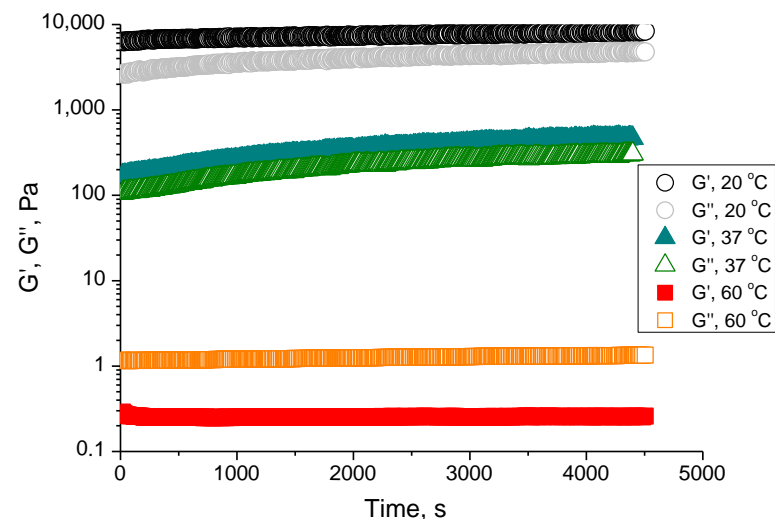


Figure 6. Shear moduli as a function of time during the crosslinking reaction of PCL-45HBPG/1SiHBPG at 20 °C, 37 °C, and 60 °C.

Figure 7 shows the variations in the elastic moduli with time for the more hydrophilic PCL-56HBPG/1SiHBPG and PCL-73HBPG/1SiHBPG at 20 °C. In the early stages, both moduli were low and the elastic portion G' was much smaller than the viscous portion, G'' . This is a characteristic of a polymeric liquid. As the time progressed, G' started to increase but no crossover was observed and the behavior of the dispersion remained viscous over the entire time of the experiment.

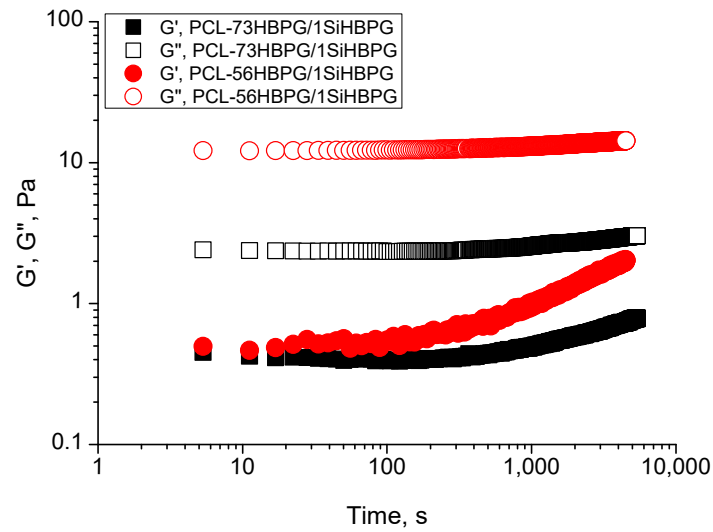


Figure 7. PCL-73HBPG/1SiHBPG and PCL-56HBPG/1SiHBPG (frequency = 1 Hz, stress = 0.1 Pa) at 20 °C.

2.3. SAXS Analysis

To investigate further the internal structure of the PCL-HBPG/1SiHBPG particles, their interaction with the solvent, and the possible structural arrangement as the concentration increases, we used SAXS at temperature ranges between 25 and 60 °C and a concentration of 1 mg/mL. The diluted dispersions of these copolymers have been analyzed using SAXS and SLS previously [24]. Representative SAXS profiles for 1 mg/mL aqueous dispersions of PCL-45HBPG/1SiHBPG at 25 °C and 60 °C and for PCL-56HBPG/1SiHBPG, PCL-73HBPG/1SiHBPG, and PCL-90HBPG/1SiHBPG at 30 °C are shown in Figure 8a,b, respectively.

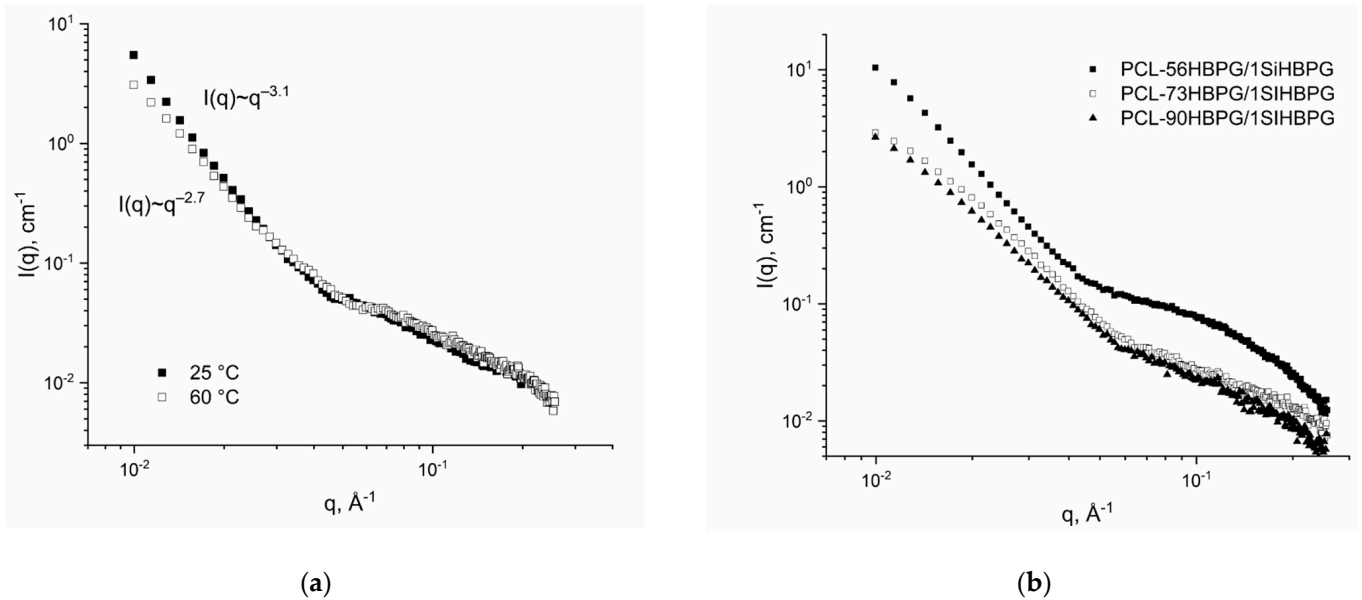


Figure 8. SAXS profiles for (a) 1 mg/mL PCL-45HBPG/1SiHBPG at 25 °C and 60 °C; (b) 1 mg/mL PCL-56HBPG/1SiHBPG, PCL-73HBPG/1SiHBPG, and PCL-90HBPG/1SiHBPG at 30 °C.

The analysis of the scattering data started with the calculation of the slope in approximation of the scattering intensity as $I(q) \sim q^{-\alpha}$. The values of the slopes at low q ranges ($<0.03 \text{ \AA}^{-1}$) are presented in Table 1. In the present setup of the SAXS experiment, it is impossible to observe scattering from large particles as a whole and the value of the slope is used to determine the internal organization of these particles. Only for PCL-45HBPG/1SiHBPG at 25 °C was the value of the slope in the range $3 < \alpha < 4$, which indicates surface fractal organization (i.e., compact core and fractal surface). For all other systems the slope was $\alpha \leq 3$, which indicates a volume fractal (non-compact structure) organization of the large particles [32]. Most probably these structural changes are responsible for the lack of elastic properties of the solutions of the more hydrophilic polymers. For a q range above 0.05 \AA^{-1} , a plateau in the scattering intensities is observed. This corresponds to scattering of objects with scale lengths less than 16 nm. They could be considered as PCL domains. The typical indication of scattering of Gaussian chains (slope-2 at a large q range) is not present, which suggests that there is a complete self-association of the copolymer chains. In this case, PCL domains provide the main contribution to the scattering intensities.

Table 1. The slope values for 1 mg/mL aqueous dispersions at 25, 30, and 60 °C.

Sample	T (°C)	Slope
PCL-45HBPG/1SiHBPG	25	3.10 ± 0.01
PCL-45HBPG/1SiHBPG	60	2.70 ± 0.01
PCL-56HBPG/1SiHBPG	30	2.90 ± 0.01
PCL-73HBPG/1SiHBPG	30	2.71 ± 0.01
PCL-90HBPG/1SiHBPG	30	2.67 ± 0.03

The scattering data at intermediate and large q ($q > 0.06 \text{ \AA}^{-1}$) were obtained by comparison with scattering from a model of an ellipsoid with the rotation axes a and b . The values of the parameters of the ellipsoid for all copolymers studied are presented in Table 2.

Table 2. Results of SAXS analysis of large q part (parameters of ellipsoid, R_g , and $I(0)$) of PCL-HBPG/1SiHBPG copolymer particles formed in 1 mg/mL aqueous solutions at 25, 30, and 60 °C.

Sample	T, °C	a, Å	b, Å	R_g , Å	V, Å ³	N_{aggPCL}
PCL-45HBPG/1SiHBPG	25	57 ± 14	18 ± 1	28	77,320	25
PCL-45HBPG/1SiHBPG	60	47 ± 5	4.3 ± 1.9	21	3640	2
PCL-56HBPG/1SiHBPG	30	29 ± 1	8.3 ± 0.7	14	8368	3
PCL-70HBPG/1SiHBPG	30	56 ± 19	4.7 ± 2.2	25	5182	2
PCL-90HBPG/1SiHBPG	30	59 ± 32	6.1 ± 3.9	27	9196	3

The domain volumes, V , were calculated using the values of a and b (Table 2) and were further used to estimate the number of PCL chains in one domain; this is the aggregation number of PCL (N_{aggPCL}). To obtain this value, the volume of the ellipsoid was divided by the volume of a PCL chain. Here, we have assumed that domains consist only of PCL chains and 100% of the PCL is in the domain, as described previously [24]. We anticipate that there will be some penetration of the 1SiHBPG moieties on the basis of the hydrophobicity of the materials. The molecular weight and density of the PCL diol was used to calculate the N_{agg} . A volume of 3100 \AA^3 was calculated to contain approximately 18 caprolactone units. The N_{aggPCL} shows a maximum value for PCL-45HBPG/1SiHBPG at 25 °C and remains largely unaffected by the increase in the HBPG/1SiHBPG content for the more hydrophilic polymers, i.e., those with higher proportions of HBPG. Furthermore, the PCL domains become considerably more elongated upon increasing the hydrophilic HBPG/1SiHBPG content, which is evident from the large increase in the anisotropy (Table 2).

2.4. Hydrolytic Disassembly of the PCL-HBPG/1SiHBPG Gels

The ester bonds in the PCL-HBPG/1SiHBPG scaffolds are biodegradable. The biodegradability properties of the new PCL-HBPG/1SiHBPG-containing crosslinked particle gels

were tested using lipase. Lipase is a naturally occurring enzyme agent which is present throughout the human body. The normal concentration range of lipase in the blood of a healthy adult under the age of 60 is 8–78 U/L [33]. The concentration of lipase that we have used in our experiment is ~100 U/L, which is comparable to that found in human serum. Lipase can catalyze the hydrolysis of lipids and has many applications [34,35]. To study the enzymatic degradation of PCL and its derivatives, pseudomonas lipase has often been utilized [36]. The addition of a 5% solution of lipase (intracellular concentration) to PCL-45HBPG/1SiHBPG resulted in large decreases in the gel's elasticities. The gel-to-fluid transitions of the PCL-45HBPG/1SiHBPG networks following the addition of lipase are shown in Figure 9. The addition of lipase resulted in network breakdown after 8 min. After this time the gel was flowing, with viscous properties being dominant ($G' < G''$). The siloxane (Si–O–Si) bond is robust, chemically resistant, and easily established [37]. We do not expect that it would degrade hydrolytically upon addition of lipase. Considering the low concentration of Si–O–Si crosslinks in PCL-HBPG/1SiHBPG, the biodegradation of the PCL portion of the gels will be solely responsible for the decreases in the gel elasticities upon addition of lipase.

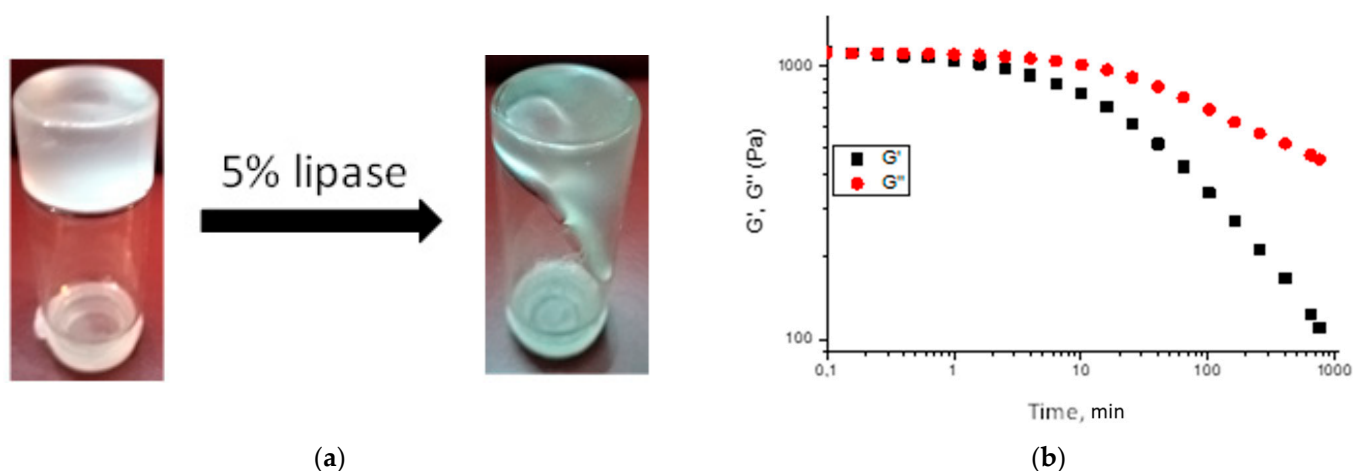


Figure 9. (a) Photographs of the PCL-45HBPG/1SiHBPG gel before and after the addition of lipase; (b) hydrolytic disassembly of the PCL-45HBPG/1SiHBPG gel by addition of 5% solution of lipase.

2.5. Biocompatibility Studies with PCL-HBPG/1SiHBPG

The response of immortalized human chondrocyte cells to the addition of PCL-HBPG/1SiHBPG was measured by using the MTT cell viability assay. Selected samples of PCL-HBPG/1SiHBPG, e.g., PCL-90HBPG/1SiHBPG and HBPG/1SiHBPG, with total weights of 20 mg were added into the well inserts for 24 h, 48 h, and 7 days. The wells were seeded with 6×10^4 immortalized human chondrocyte cells with a total cell culture volume of 1 mL. The cell media were in direct contact with the copolymer dispersions, which were used as received, without additional purification before use. The results indicated the absence of any significant cell disruption after 48 h of direct contact with the samples (Figure 10). The cell viability was maintained up to 75% after 7 days of direct exposure of the cells to the samples. The cells were still elongated and attached after 7 days of incubation. Representative optical micrographs of the cells taken after 7 days incubation with HBPG/1SiHBPG and PCL-90HBPG/1SiHBPG gels are shown in Figure 11b,c, respectively. The data are compared to control images (Figure 11a) which show cell regions that were not exposed to the gels. The cytotoxicity results revealed that our new HBPG/1SiHBPG and PCL-HBPG/1SiHBPG copolymers show very good biocompatibility, with at least 75% cell viability after 7 days of incubation.

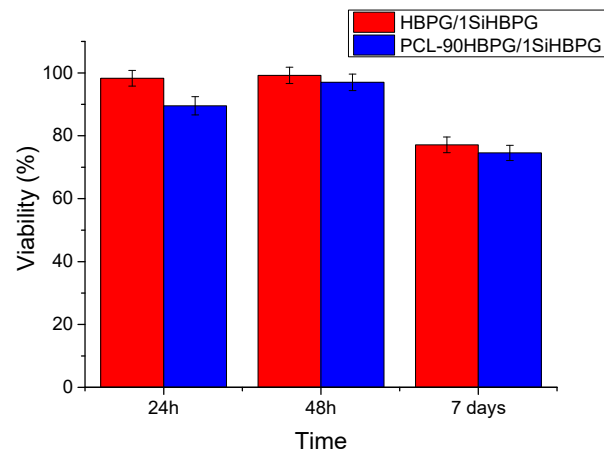


Figure 10. MTT assay for HBPG/1SiHBPG and PCL-90HBPG/1SiHBPG. Cell viability was calculated as a percentage relative to a control sample.

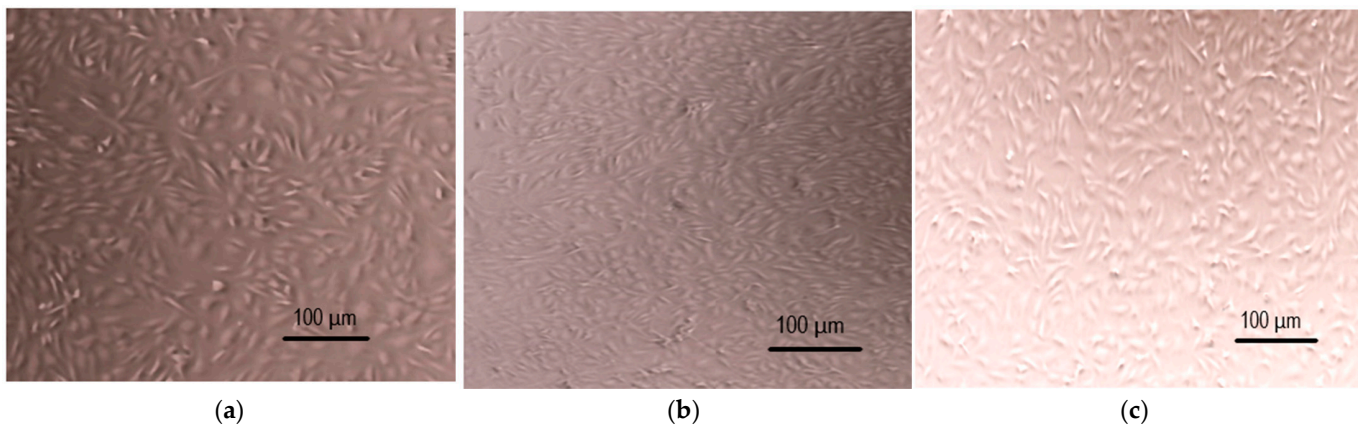


Figure 11. Optical micrographs of (a) chondrocytes that were not in contact with the gel (control); (b) chondrocyte cells that were in contact with HBPG/1SiHBPG, and (c) chondrocyte cells that were in contact with PCL-90HBPG/1SiHBPG, taken after 7 days of incubation.

3. Discussion

Structure–Properties Relationship in PCL-HBPG/1SiHBPG Concentrated Polymer Dispersions

In our studies, we applied a completely new approach for the development of trimethoxysilyl-capped HBPG/PCL-based gel scaffolds. The gels were derived in two steps: firstly, the physical gels were formed from a concentrated dispersion of PCL-HBPG/1SiHBPG particles. In the second step, the physical network was locked in place due to the gradual hydrolysis (and subsequent Si–O–Si crosslink formation) of trimethoxysilyl groups. Our investigation clearly shows that variations in the PCL block length and the copolymer concentration can result in large differences in both the properties and performance of the new PCL-HBPG/1SiHBPG systems. In aqueous dispersion above the CAC, the PCL-HBPG/1SiHBPG system self-assembled and formed large multicore particles composed of compact PCL domains and an HBPG/1SiHBPG corona hydrated in water. The weight average molar masses (M_w) and the corresponding aggregation numbers (N_{agg}), radii of gyration (R_g), and second virial coefficients (A_2) of the PCL-HBPG/1SiHBPG particles formed in aqueous solution were determined by static light scattering, as described previously [24]. Herein, we use SAXS to investigate the internal structure of the large PCL-HBPG/1SiHBPG particles formed from the copolymers in the regime of higher concentrations. The SAXS intensities were described by a model of an ellipsoid of rotation axes a and b . The R_g values of the domains are presented in Table 2. The values of the parameters of the ellipsoid were used to determine the domain volumes, V , and their aggregation number (N_{agg}). For the more hydrophobic PCL-45HBPG/1SiHBPG, in the regime

of high concentrations and low temperatures, the large particles fuse, the PCL domains are in closer proximity because of the increasing concentration, and they are arranged into compact structures surrounded by polar HBPG/1SiHBPG branches (Figure 12a). This is evidenced by them having the largest domain volume and their N_{agg} observed for PCL-45HBPG/1SiHBPG at 25 °C. The SAXS data also suggested a structural transformation of the PCL domains from surface fractal structures (compact core and rough surface) to volume fractal (non-compact core and rough surface) for the concentrated dispersion of PCL-45HBPG/1SiHBPG at 60 °C and for the more hydrophilic PCL-73HBPG/1SiHBPG, PCL-56HBPG/1SiHBPG, and PCL-90HBPG/1SiHBPG at 30 °C (Figure 12b). The increase in the anisotropy of the PCL core upon increasing the hydrophilic content could be attributed to the geometric packing consideration, which affects the aggregate shape transition, as discussed previously in analogous systems [38].

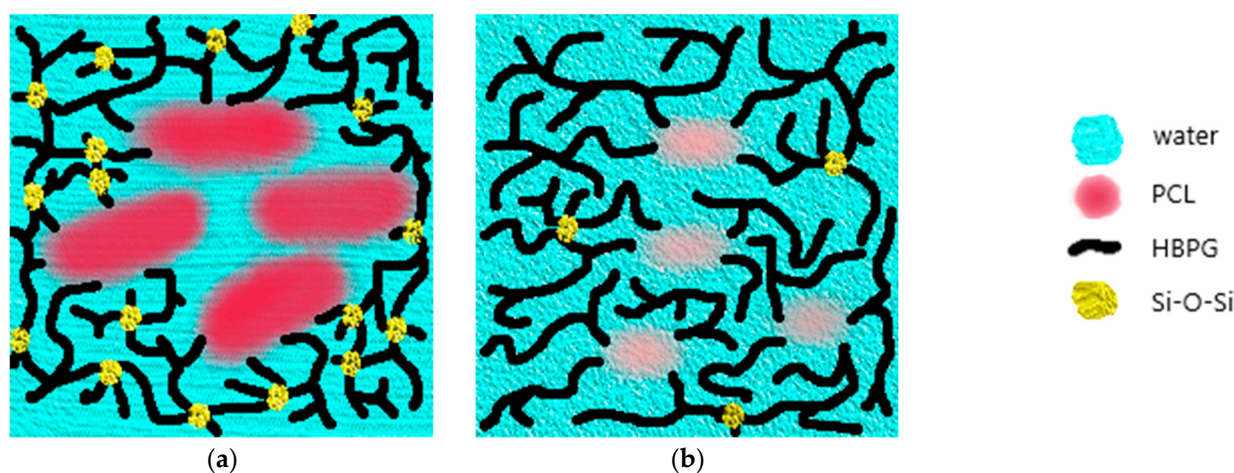


Figure 12. Schematic presentation of the changes in the internal structure of the particles formed by (a) PCL-45HBPG/1SiHBPG in concentrated solutions at 25 °C and (b) PCL-45HBPG/1SiHBPG at 60 °C and hydrophilic PCL-56HBPG/1SiHBPG, PCL-73HBPG/1SiHBPG, and PCL-90HBPG/1SiHBPG at 30 °C.

For the PCL-HBPG/1SiHBPG systems, the sol–gel phase transition was only observed for PCL-45HBPG/1SiHBPG at temperatures below 40 °C. The sol phase is defined as a flowing fluid, whereas the gel phase is elastic and maintains its integrity. The physical gels were formed by crosslinking the interpenetrating particle shells via numerous inter- and intramolecular hydrogen bonds formed within the HBPG/1SiHBPG moieties as well as the ability of the PCL to diffuse into the different domains. As the temperature increased, the G'' and G' moduli values were found to sharply decrease and PCL-45HBPG/1SiHBPG displayed a liquid-like behavior, with $G'' > G'$. The collapse of physical crosslinkages could be attributed to the increased solubility of the HBPG/1SiHBPG branches as the temperature increases [24]. For the PCL-HBPG/1SiHBPG systems, the delicate balance between the hydrophobic and hydrophilic portions of the copolymers determines the macroscopic behavior of the crosslinked networks in their aqueous solutions. For PCL-45HBPG/1SiHBPG, the changes in temperature caused changes in the interactions between the hydrophilic and hydrophobic polymer segments with water, which in turn had an effect upon the solubility of the crosslinked network, as seen for other analogous systems [39]. The elastic properties of PCL-45HBPG/1SiHBPG at 25 °C could be attributed to the hydrophobic interaction between the PCL segments and the numerous hydrogen bonds formed between the HBPG/1SiHBPG moieties. The increases in temperature and the hydrophilic content resulted in the disintegration of the PCL domains. This is evidenced by a decrease in the volume of the PCL domains and their aggregation number as the temperature and the relative hydrophilic content of the polymer increased.

The concentrated dispersions of PCL-73HBPG/1SiHBPG, PCL-56HBPG/1SiHBPG, and PCL-90HBPG/1SiHBPG behaved as fluids over the entire temperature range tested, with $G'' > G'$. This finding suggests that the macroscopic behavior of the PCL-HBPG/1SiHBPG systems is largely determined by the size of the PCL domains. The latter interact via HBPG/1SiHBPG chains of varying length grafted onto their surface. The PCL hydrophobic domains, bonded to the long hydrophilic chains, function as stickers, which intermolecularly associate through hydrophobic interactions. The effect which a hydrophobic spacer exerts upon a gel's properties within a multicomponent system has been previously reported [39]. It has been shown that an increase in the length of the hydrophobic chain significantly influences both the microstructure and mechanical properties as well as the underlying molecular packing in copolymer co-assemblies. Our studies suggest that the stronger hydrophobic interactions between the PCL domains in the more hydrophobic PCL-45HBPG/1SiHBPG increase the interparticle interactions and promote copolymer gelation under physiological temperature conditions.

The time-dependent rheological measurements of the PCL-45HBPG/1SiHBPG gels showed a gradual increase in the gel's mechanical strength over time as the extent of methoxysilane hydrolysis and crosslinking proceeded. Increases in the G' and G'' values over time were also observed for the rest of the PCL-HBPG/1SiHBPG systems. This finding could be attributed to the inter- and intra-shell crosslinking of the copolymer particles because of the gradual hydrolysis of the trimethoxysilyl groups, which generate silanol moieties that readily condense to form strong Si–O–Si bonds, thereby crosslinking the particles (Figure 12).

The hydrogels intended for soft tissue regeneration should feature excellent biocompatibility, facile biodegradability, high stability, and favorable mechanical properties for 3D cell culture [2]. To control the biodegradation it is essential to utilize the proteolytic degradation mechanisms which operate in the ECM. ECM proteins such as collagen, laminin, and fibrin are readily degraded by enzymes at cleavage sites. The incorporation of polyester segments within synthetic hydrogels has been used to facilitate the resulting scaffold's biodegradation [40,41]. Nguyen et al. [42] developed a biodegradable hydrogel scaffold based on poly(propylene fumarate-co-ethylene glycol) and encapsulated endothelial cells in the gels for vascular cell growth. Their study demonstrated that in biodegradable hydrogel scaffolds, the cells were spread throughout the hydrogel scaffold and attained an increase in both their ECM production and proliferation rate compared to cells in non-degradable scaffolds. In our PCL-HBPG/1SiHBPG systems, the ester groups of polycaprolactone are biodegradable and their enzymatic degradation has often been achieved using lipase [43]. The PCL degrades upon hydrolysis, eventually being broken down into oligomers or monomers that are subjected to natural metabolic processes. Accordingly, a solution of lipase in phosphate-buffered saline was used to trigger the biodegradation of the gel scaffolds in this project. The new gels derived from the PCL-45HBPG/1SiHBPG-containing crosslinked particles possessed excellent biodegradability. Less than eight minutes was required for the gel to turn to a liquid following exposure to lipase. It is proposed that enzyme-triggered disassembly of the scaffold will provide space for the final stage of tissue reconstruction and the growth of ECM into the space provided. The rate and extent of biodegradation are essential factors in the design of tissue scaffolds. For successful tissue repair, it is important that the rate of biodegradation coincides with the rate of new tissue formation. Once it is implanted, the scaffold's degradation should occur in a timely manner to enable appropriate remodeling of the tissue. In the event that biodegradation occurs more rapidly than the tissue regeneration, the corresponding scaffolds will be unable to provide mechanical support and promote the tissue growth; on the other hand, if the biodegradation progresses too slowly, then tissue regeneration will be prevented [40,41]. The PCL-HBPG/1SiHBPG gel scaffolds display a faster degradation rate. The rate of hydrolysis of the ester linkages is accelerated by the increase in water penetration. The ability of water to penetrate the polymer chain depends on the polymer's glass transition temperature and crystallinity [41]. The highest T_g values have been previously reported for

the more hydrophobic PCL-45HBPG/1SiHBPG [24]. The high T_g is attributed to comparatively low molecular motion and limited free volume in the polymer network. To improve the rate of hydrolytic disintegration of PCL-45HBPG/1SiHBPG a simple manipulation of the reactant stoichiometry and functionality could be performed. For example, the polymer chain could be stiffened via the incorporation of bulky side groups or it could be made more hydrophobic. A high degree of crosslinking or chain branching could also limit water penetration and improve biodegradability [44].

Another important requirement of any biomaterial is biocompatibility. A wide variety of synthetic polyesters have been shown to be biocompatible in the body [41]. Polycaprolactone has been used in a range of medical applications such as degradable sutures, stents, and wound dressings, all of which have acquired FDA approval [45]. PCL-HBPG/1SiHBPG showed good biocompatibility. The MTT cell viability was maintained at up to 75% after 7 days of direct exposure of immortalized human chondrocyte cells with the gels. The cells preserved their elongated morphology and were still attached after 7 days of incubation. To improve biocompatibility, the gel chemistry of PCL-HBPG/1SiHBPG can be altered with the addition of certain molecules or monomers [46]. For example, the incorporation of adhesion proteins into the polymer scaffold can support the differentiation, proliferation, and migration, and even improve cell survival rates [41,47]. Alternatively, polymer chain ends can be functionalized to enable grafting of biochemicals [48]. The presence of multiple hydroxyl groups within HBPG provides the opportunity for functionalization and attachment to targeted biological cells and tissues. The ability of the gels to decompose into non-toxic and low-molecular-weight species that could be metabolized and/or readily excreted from the body encourages application of the PCL-HBPG/1SiHBPG materials in drug delivery.

The physical properties of a gel scaffold should closely resemble those at the target site, so that it can withstand the forces acting on it. The extent of crosslinking is an important factor which affects the mechanical properties of the scaffold. Too many crosslinks lead to a brittle structure, whereas too few will produce a material that is not strong enough to provide the support which is necessary [41]. Physical gels are weaker than chemical gels and even with optimization may lack the required mechanical properties for tissue regeneration. For PCL-HBPG/1SiHBPG, the extent of covalent crosslinking is in the range of 0.3 to 0.7 mol%, which should be optimized to display mechanical properties resembling those of the target tissue. Tensile testing up to or past the yield or failure point is not easily performed on weak gels and networks because it is difficult to avoid debonding of the sample from the test geometry [49]. The mechanical properties of the novel gels based on the PCL-HBPG/1SiHBPG copolymers have been studied using rheology. Rheological techniques and methods have been employed successfully for many decades in the characterization of polymers and biomaterials [50].

4. Materials and Methods

4.1. Materials

The copolymers used in the present study were synthesized as described elsewhere [22] and characterized by ^1H NMR, gel permeation chromatography, thermogravimetric analysis (TGA), and dynamic scanning calorimetry (DSC). They feature a constant molar mass of the PCL middle block and HBPG/1SiHBPG contents varying from 45 to 90 mol% for the HBPG and from 0.6 to 1.4 mol% for the SiHBPG. Their aqueous solution properties were investigated by dye solubilization, turbidimetry, light scattering, and SAXS.

4.2. Sample Preparation

Aqueous solutions in the concentration range from 1 mg/mL were prepared gravimetrically by adding water to a pre-weighed quantity of the copolymer. The solution was then stirred at room temperature for 24 h.

4.3. Methods and Analysis

Rheology measurements were carried out at temperatures from 20 to 60 °C using a HR-1 Discovery Hybrid Rheometer with a 250 µm gap and a 20 mm diameter steel plate. All strain-sweep measurements were conducted at a frequency of 1 Hz. All frequency-sweep measurements were carried out at a strain of 0.1%. The SAXS experiments were completed with a laboratory SAXS instrument (Nanostar, Bruker AXS GmbH, Karlsruhe, Germany) which uses an IµS micro-focus X-ray source with a power of 30 W, utilizing the wavelength of the Cu Kα line. The detector used was a VÅNTEC-2000 (14 × 14 cm² and 2048 × 2048 pixels). The distance from sample to detector was 108.3 cm and the accessible q range was between 0.008 and 0.23 Å⁻¹. Samples were placed into glass capillaries of 2 mm diameter with the temperature controlled (ΔT = 0.1 K). The standard data reduction procedure was applied, which includes correction for the background scattering of the solvent measured in a capillary of equal size, and then the scattering intensities were converted to absolute units using the scattering of pure water measured in a 2 mm capillary at 20 °C.

4.4. Gel Cytotoxicity Studies

T/C28a2 cells (Merck, Rahway, NJ, USA, 1 × 10⁶ cells/vial), immortalized human chondrocyte cell, were cultured in Dulbecco's modified Eagle's medium (DMEM, Gibco, Waltham, MA, USA) supplemented with 10% fetal bovine serum (FBS, Gibco) and antibiotic/antimycotic (Sigma-Aldrich, Gillingham, UK) at 37 °C in a CO₂ atmosphere. The T/C-28a2 cell line was established by transfecting primary cultures (day 5) of costal cartilage from a 15-year-old female with a retroviral vector expressing simian virus SV40 large T antigen. Cells were seeded at a density of 6 × 10⁴ per well onto well plates containing 0.4 µm cell-culture inserts (BD Biosciences, Franklin Lakes, NJ, USA) and allowed to adhere overnight before exposure to 20 mg of PCL-HBPG/1SiHBPG concentrated particle dispersions. Cell viability was calculated as a percentage relative to a control sample and was measured at 24 h, 48 h, and 7-day time-points using an MTT assay (Merck Life Science UK Limited, Gillingham, Dorset, UK) as per the manufacturer's instructions.

4.5. Scaffold Degradation Studies

The biodegradation studies were carried out by the addition of 100 µL of 5% lipase (lipase powder ~200 U/g from *Aspergillus niger*) solution in 10 mL of phosphate-buffered saline (pH 7.4) to the gel (150 mg) at 37 °C. The resulting concentration of lipase is comparable to that found in human serum. The test tubes containing the samples were shaken at 70 rpm for two minutes before the measurements.

5. Conclusions

In this study, we investigate the relationship between the structure, mechanical properties, and performance of the novel PCL-HBPG/1SiHBPG gel scaffolds that have been developed for soft tissue regeneration. A variety of characterization methods, including small-angle X-ray scattering, optical microscopy, and dynamic rheology have been used to investigate their aqueous solution properties at higher concentrations of 1 mg/mL. We applied a completely new approach for the development of the scaffolds. In the first step, the physical gels were formed by crosslinking the interpenetrating shells of the PCL-HBPG/1SiHBPG particles via numerous inter- and intramolecular hydrogen bonds formed within the HBPG/1SiHBPG moieties as well as the ability of the PCL to diffuse into the different domain. In the second step, the physical network was locked in place due to the gradual hydrolysis (and subsequent Si–O–Si crosslink formation) of trimethoxysilyl groups. Our investigation clearly shows that variations in the hydrophobic/hydrophilic portions of the copolymers determined the macroscopic properties of the PCL-HBPG/1SiHBPG systems. The sol–gel phase transition was only observed for the most hydrophobic system, PCL-45HBPG/1SiHBPG, at low temperatures. The elastic properties of PCL-45HBPG/1SiHBPG were attributed to the hydrophobic interaction between the PCL segments and the nu-

merous hydrogen bonds formed between HBPG/1SiHBPG moieties. Increases in the temperature and the hydrophilic content resulted in the disintegration of the PCL domains and the occurrence of a flow zone. The PCL-HBPG/1SiHBPG particle gels showed a steady increase in the gels' elasticity over time at low temperatures, which was attributed to the gradual crosslinking of the trimethoxysilyl groups. The PCL-45HBPG/1SiHBPG gels were biodegradable upon the addition of lipase. The cytotoxicity results with immortalized chondrocyte cells revealed that the new PCL-HBPG/1SiHBPG gels show very good biocompatibility, with at least 75% cell viability after 7 days of incubation.

Author Contributions: Conceptualization, S.S.H.; methodology, C.G.-C., V.M.G., J.H. and S.S.H.; formal analysis, C.G.-C., V.M.G. and S.S.H.; investigation, C.G.-C., V.M.G. and S.S.H.; resources, V.M.G., J.H. and S.S.H.; data curation, C.G.-C., V.M.G. and S.S.H.; writing—original draft preparation, S.S.H.; writing—review and editing, C.G.-C., V.M.G., J.H. and S.S.H.; supervision, S.S.H.; project administration, S.S.H.; funding acquisition, S.S.H. All authors have read and agreed to the published version of the manuscript.

Funding: We are grateful to the Engineering and Physical Sciences Research Council, U.K. for financial support (Award Reference: EP/M02881X/1). The SAXS study was supported by the European Commission under the sixth Framework Program through the Key Action: Strengthening the European Research Area, Research Infrastructures (Contract RII3-CT-2003-505925, Grant Agreement No. 226507-NMI3).

Data Availability Statement: Not applicable.

Acknowledgments: We thank Stanislav Rangelov, from the Institute of Polymers, Bulgarian Academy of Sciences, for critical reading and feedback provided.

Conflicts of Interest: The authors declare no conflict of interest.

References

1. Mellati, A.; Hasanzadeh, E.; Gholipourmalekabadi, M.; Enderami, S.E. Injectable Nanocomposite Hydrogels as an Emerging Platform for Biomedical Applications: A Review. *Mater. Sci. Eng. C* **2021**, *131*, 112489–112514. [[CrossRef](#)]
2. Mantha, S.; Pillai, S.; Khayambashi, P.; Upadhyay, A.; Zhang, Y.; Tao, O.; Pham, H.M.; Tran, S.D. Smart Hydrogels in Tissue Engineering and Regenerative Medicine. *Materials* **2019**, *12*, 3323. [[CrossRef](#)]
3. Spicer, C.D. Hydrogel Scaffolds for Tissue Engineering: The Importance of Polymer Choice. *Polym. Chem.* **2020**, *11*, 184–219. [[CrossRef](#)]
4. Hou, Q.; De Bank, P.A.; Shakesheff, K.M. Injectable Scaffolds for Tissue Regeneration. *J. Mater. Chem.* **2004**, *14*, 1915–1923. [[CrossRef](#)]
5. Fu, S.Z.; Ni, P.Y.; Wang, B.Y.; Chu, B.Y.; Zheng, L.; Luo, F.; Luo, J.C.; Qian, Z.Y. Injectable and Thermo-Sensitive PEG-PCL-PEG Copolymer/Collagen/n-HA Hydrogel Composite for Guided Bone Regeneration. *Biomaterials* **2012**, *33*, 4801–4809. [[CrossRef](#)]
6. Diniz, I.M.A.; Chen, C.; Xu, X.; Ansari, S.; Zadeh, H.H.; Marques, M.M.; Shi, S.; Moshaverinia, A. Pluronic F-127 Hydrogel as a Promising Scaffold for Encapsulation of Dental-Derived Mesenchymal Stem Cells. *J. Mater. Sci. Mater. Med.* **2015**, *26*, 153–163. [[CrossRef](#)]
7. Li, G.; Wu, J.; Wang, B.; Yan, S.; Zhang, K.; Ding, J.; Yin, J. Self-Healing Supramolecular Self-Assembled Hydrogels Based on Poly(l-Glutamic Acid). *Biomacromolecules* **2015**, *16*, 3508–3518. [[CrossRef](#)]
8. Payyappilly, S.; Dhara, S.; Chattopadhyay, S. Thermoresponsive Biodegradable PEG-PCL-PEG Based Injectable Hydrogel for Pulsatile Insulin Delivery. *J. Biomed. Mater. Res. Part A* **2014**, *102*, 1500–1509. [[CrossRef](#)]
9. Xue, X.; Hu, Y.; Wang, S.; Chen, X.; Jiang, Y.; Su, J. Fabrication of Physical and Chemical Crosslinked Hydrogels for Bone Tissue Engineering. *Bioact. Mater.* **2022**, *12*, 327–339. [[CrossRef](#)]
10. Calderón, M.; Quadir, M.A.; Sharma, S.K.; Haag, R. Dendritic Polyglycerols for Biomedical Applications. *Adv. Mater.* **2010**, *22*, 190–218. [[CrossRef](#)]
11. Fedorovich, N.E.; Oudshoorn, M.H.; van Geemen, D.; Hennink, W.E.; Alblas, J.; Dhert, W.J.A. The Effect of Photopolymerization on Stem Cells Embedded in Hydrogels. *Biomaterials* **2009**, *30*, 344–353. [[CrossRef](#)] [[PubMed](#)]
12. Li, J.; Li, H.; Yang, X.; Luo, P.; Wu, Z.; Zhang, X. The Supramolecular Hydrogel Based on Hyperbranched Polyglycerol and Dextran as a Scaffold for Living Cells and Drug Delivery. *RSC Adv.* **2015**, *5*, 86730–86739. [[CrossRef](#)]
13. de Queiroz, A.A.A.; Bressiani, J.C.; Bressiani, A.H.A.; Higa, O.Z.; Abraham, G.A. A Novel Bone Scaffolds Based on Hyperbranched Polyglycerol Fibers Filled with Hydroxyapatite Nanoparticles: In Vitro Cell Response. *Key Eng. Mater.* **2008**, *396–398*, 633–636. [[CrossRef](#)]

14. Wu, C.; Strehmel, C.; Achazi, K.; Chiappisi, L.; Dervedde, J.; Lensen, M.C.; Gradzielski, M.; Ansorge-Schumacher, M.B.; Haag, R. Enzymatically Cross-Linked Hyperbranched Polyglycerol Hydrogels as Scaffolds for Living Cells. *Biomacromolecules* **2014**, *15*, 3881–3890. [[CrossRef](#)]
15. Haryanto; Singh, D.; Huh, P.H.; Kim, S.C. Hyperbranched Poly(Glycidol)/Poly(Ethylene Oxide) Crosslinked Hydrogel for Tissue Engineering Scaffold Using e-Beams. *J. Biomed. Mater. Res. Part A* **2016**, *104*, 48–56. [[CrossRef](#)]
16. John, L.; Janeta, M.; Rajczakowska, M.; Ejfler, J.; Lydzba, D.; Szafert, S. Synthesis and Microstructural Properties of the Scaffold Based on a 3-(Trimethoxysilyl)Propyl Methacrylate–POSS Hybrid towards Potential Tissue Engineering Applications. *RSC Adv.* **2016**, *6*, 66037–66047. [[CrossRef](#)]
17. Li, P.; Luo, Z.; Li, X.; Wang, R.; Chen, H.; Zhao, Y.; Wang, J.; Huang, N. Preparation, Evaluation and Functionalization of Biomimetic Block Copolymer Coatings for Potential Applications in Cardiovascular Implants. *Appl. Surf. Sci.* **2020**, *502*, 144085. [[CrossRef](#)]
18. Linn, J.D.; Liberman, L.; Neal, C.A.P.; Calabrese, M.A. Role of Chain Architecture in the Solution Phase Assembly and Thermoreversibility of Aqueous PNIPAM/Silyl Methacrylate Copolymers. *Polym. Chem.* **2022**, *13*, 3840–3855. [[CrossRef](#)]
19. Zheng, Z.; Huang, J.; Gao, X.; Luo, Y. Semi-Spontaneous Post-Crosslinking Triblock Copolymer Electrolyte for Solid-State Lithium Battery. *Batteries* **2023**, *9*, 465. [[CrossRef](#)]
20. Osváth, Z.; Tóth, T.; Iván, B. Sustained Drug Release by Thermoresponsive Sol–Gel Hybrid Hydrogels of Poly(N-Isopropylacrylamide-Co-3-(Trimethoxysilyl)Propyl Methacrylate) Copolymers. *Macromol. Rapid Commun.* **2017**, *38*, 1600724. [[CrossRef](#)]
21. Osváth, Z.; Tóth, T.; Iván, B. Synthesis, Characterization, LCST-Type Behavior and Unprecedented Heating-Cooling Hysteresis of Poly(N-Isopropylacrylamide-Co-3-(Trimethoxysilyl)Propyl Methacrylate) Copolymers. *Polymer* **2017**, *108*, 395–399. [[CrossRef](#)]
22. Fan, X.; Gu, S.; Wu, L.; Yang, L. Preparation and Characterization of Thermoresponsive Poly(N-Isopropylacrylamide) Copolymers with Enhanced Hydrophilicity. *e-Polymers* **2020**, *20*, 561–570. [[CrossRef](#)]
23. Du, J.; Armes, S.P. PH-Responsive Vesicles Based on a Hydrolytically Self-Cross-Linkable Copolymer. *J. Am. Chem. Soc.* **2005**, *127*, 12800–12801. [[CrossRef](#)] [[PubMed](#)]
24. González-Chomón, C.; Garamus, V.M.; Rangelov, S.; Ebdon, J.R.; Novakov, C.; Halacheva, S.S. Trimethoxysilyl End-Capped Hyperbranched Polyglycidol/Polycaprolactone Copolymers for Cell Delivery and Tissue Repair: Synthesis, Characterisation and Aqueous Solution Properties. *Eur. Polym. J.* **2019**, *112*, 648–659. [[CrossRef](#)]
25. Indumathy, B.; Sathiyathan, P.; Prasad, G.; Reza, M.S.; Prabu, A.A.; Kim, H. A Comprehensive Review on Processing, Development and Applications of Organofunctional Silanes and Silane-Based Hyperbranched Polymers. *Polymers* **2023**, *15*, 2517. [[CrossRef](#)] [[PubMed](#)]
26. Serman, S.; Marsden, J.G. Silane Coupling Agents. *Ind. Eng. Chem.* **1966**, *58*, 33–37. [[CrossRef](#)]
27. Halacheva, S.; Rangelov, S.; Tsvetanov, C. Rheology of Aqueous Solutions of Polyglycidol-Based Analogues to Pluronic Block Copolymers. *J. Phys. Chem. B* **2008**, *112*, 1899–1905. [[CrossRef](#)]
28. Ciriminna, R.; Fidalgo, A.; Pandarus, V.; Béland, F.; Ilharco, L.M.; Pagliaro, M. The Sol–Gel Route to Advanced Silica-Based Materials and Recent Applications. *Chem. Rev.* **2013**, *113*, 6592–6620. [[CrossRef](#)]
29. Avnir, D.; Coradin, T.; Lev, O.; Livage, J. Recent Bio-Applications of Sol–Gel Materials. *J. Mater. Chem.* **2006**, *16*, 1013–1030. [[CrossRef](#)]
30. Arkles, B.; Steinmetz, J.; Zazyczny, J.; Mehta, P. Factors Contributing to the Stability of Alkoxysilanes in Aqueous Solution. *J. Adhes. Sci. Technol.* **1992**, *6*, 193–206. [[CrossRef](#)]
31. Bianco, S.; Panja, S.; Adams, D.J. Using Rheology to Understand Transient and Dynamic Gels. *Gels* **2022**, *8*, 132. [[CrossRef](#)]
32. Avnir, D.; Gutfraind, R.; Farin, D. Fractal Analysis in Heterogeneous Chemistry. In *Fractals in Science*; Bunde, A., Havlin, S., Eds.; Springer: Berlin/Heidelberg, Germany, 1994; pp. 229–256. ISBN 978-3-642-77953-4.
33. Ko, J.; Cho, J.; Petrov, M.S. Low Serum Amylase, Lipase, and Trypsin as Biomarkers of Metabolic Disorders: A Systematic Review and Meta-Analysis. *Diabetes Res. Clin. Pract.* **2020**, *159*, 107974. [[CrossRef](#)] [[PubMed](#)]
34. Brockman, H.L. Lipases. In *Encyclopedia of Biological Chemistry*, 2nd ed.; Academic Press: Cambridge, MA, USA, 2013; pp. 729–732.
35. Singh, R.S.; Singh, T.; Pandey, A. Microbial Enzymes—An Overview. In *Advances in Enzyme Technology*, 1st ed.; Elsevier: Amsterdam, The Netherlands, 2019; pp. 1–40.
36. Blackwell, C.J.; Haernvall, K.; Guebitz, G.M.; Groombridge, M.; Gonzales, D.; Khosravi, E. Enzymatic Degradation of Star Poly(ϵ -Caprolactone) with Different Central Units. *Polymers* **2018**, *10*, 1266. [[CrossRef](#)]
37. Glosz, K.; Stolarczyk, A.; Jarosz, T. Siloxanes—Versatile Materials for Surface Functionalisation and Graft Copolymers. *Int. J. Mol. Sci.* **2020**, *21*, 6387. [[CrossRef](#)] [[PubMed](#)]
38. Nagarajan, R. Constructing a Molecular Theory of Self-Assembly: Interplay of Ideas from Surfactants and Block Copolymers. *Adv. Colloid Interface Sci.* **2017**, *244*, 113–123. [[CrossRef](#)] [[PubMed](#)]
39. Panja, S.; Dietrich, B.; Trabold, A.; Zydell, A.; Qadir, A.; Adams, D.J. Varying the Hydrophobic Spacer to Influence Multicomponent Gelation. *Chem. Commun.* **2021**, *57*, 7898–7901. [[CrossRef](#)] [[PubMed](#)]
40. Zhu, J.; Marchant, R.E. Design Properties of Hydrogel Tissue-Engineering Scaffolds. *Expert Rev. Med. Devices* **2011**, *8*, 607–626. [[CrossRef](#)]
41. Place, E.S.; George, J.H.; Williams, C.K.; Stevens, M.M. Synthetic Polymer Scaffolds for Tissue Engineering. *Chem. Soc. Rev.* **2009**, *38*, 1139–1151. [[CrossRef](#)]

42. Nguyen, K.T.; West, J.L. Photopolymerizable Hydrogels for Tissue Engineering Applications. *Biomaterials* **2002**, *23*, 4307–4314. [[CrossRef](#)]
43. Chen, D.R.; Bei, J.Z.; Wang, S.G. Polycaprolactone Microparticles and Their Biodegradation. *Polym. Degrad. Stab.* **2000**, *67*, 455–459. [[CrossRef](#)]
44. Cushing, M.C.; Anseth, K.S. Hydrogel Cell Cultures. *Science* **2007**, *316*, 1133–1134. [[CrossRef](#)] [[PubMed](#)]
45. Manoukian, O.S.; Arul, M.R.; Sardashti, N.; Stedman, T.; James, R.; Rudraiah, S.; Kumbar, S.G. Biodegradable Polymeric Injectable Implants for Long-Term Delivery of Contraceptive Drugs. *J. Appl. Polym. Sci.* **2018**, *135*, 46068. [[CrossRef](#)]
46. Aurand, E.R.; Wagner, J.; Lanning, C.; Bjugstad, K.B. Building Biocompatible Hydrogels for Tissue Engineering of the Brain and Spinal Cord. *J. Funct. Biomater.* **2012**, *3*, 839–863. [[CrossRef](#)] [[PubMed](#)]
47. Zeng, J.; Aigner, A.; Czubayko, F.; Kissel, T.; Wendorff, J.H.; Greiner, A. Poly(Vinyl Alcohol) Nanofibers by Electrospinning as a Protein Delivery System and the Retardation of Enzyme Release by Additional Polymer Coatings. *Biomacromolecules* **2005**, *6*, 1484–1488. [[CrossRef](#)] [[PubMed](#)]
48. Gonen-Wadmany, M.; Oss-Ronen, L.; Seliktar, D. Protein–Polymer Conjugates for Forming Photopolymerizable Biomimetic Hydrogels for Tissue Engineering. *Biomaterials* **2007**, *28*, 3876–3886. [[CrossRef](#)]
49. Picout, D.R.; Ross-Murphy, S.B. Rheology of Biopolymer Solutions and Gels. *Sci. World J.* **2003**, *3*, 105–121. [[CrossRef](#)] [[PubMed](#)]
50. Murata, H. *Rheology—Theory and Application to Biomaterials*; Gomes, A.D.S., Ed.; IntechOpen: Rijeka, Yugoslavia, 2012; Chapter 17; pp. 403–426.

Disclaimer/Publisher’s Note: The statements, opinions and data contained in all publications are solely those of the individual author(s) and contributor(s) and not of MDPI and/or the editor(s). MDPI and/or the editor(s) disclaim responsibility for any injury to people or property resulting from any ideas, methods, instructions or products referred to in the content.